Supplementary Information

Optical fibre long-period grating sensors modified with antifouling bio-functional nano-brush

Markéta Vrabcová [a,b], Monika Spasovová [a,b], Michala Forinová [a,b], Ambra Gianetti [c], Milan Houska [a], N. Scott Lynn Jr. [a], Francesco Baldini [c], Jaromír Kopeček [a], Francesco Chiavaioli [c,*], and Hana Vaisocherová-Lísalová [a,*]

[a] FZU – Institute of Physics, Czech Academy of Sciences, Na Slovance 2, Prague 182 00, Czechia

[b] Institute of Physics, Faculty of Mathematics and Physics, Charles University, Ke Karlovu 3, Prague, 121 16, Czechia

[c] Institute of Applied Physics "Nello Carrara", National Research Council of Italy, Via Madonna del Piano 10, 50019 Sesto Fiorentino, Firenze, Italy

* Corresponding authors: F.C. f.chiavaioli@ifac.cnr.it, H.V.-L. lisalova@fzu.cz

Manufacturing of long-period gratings

Optical fibre long-period gratings (LPG) were fabricated in single-mode photosensitive fibres using a KrF excimer laser (Compex 110, Lambda Physics GmbH, Gottingen, Germany) and the point-to-point method.[1] Some manufacturing parameters were changed, such as the grating period from 300 µm to 370 µm, the number of laser shots per grating plane from 2000 to 2500 and the number of grating planes from 56 to 73. Fig. S1 shows the transmission spectra of five LPG fibres (labelled as LPG 1 to LPG 5) that were achieved by changing the manufacturing parameters. Typically, LPG fibres display one or more attenuation or resonance bands in the transmission spectrum that in turn correspond to the light coupling to a specific fibre cladding mode.[2] The grating period determines the modes, and hence mode orders that are excited in the fibre: the shorter the grating period is, the higher the mode order is. The modes at longer wavelengths refer to an higher mode order and usually exhibit higher sensitivity.[3] In our case, despite the different manufacturing parameters we used for each LPG fibre, the resonance band at longer wavelengths corresponds to the same mode order (7^{th}), and hence the sensors are envisaged to provide the same performance, with a volume sensitivity on the order of tens of nm RIU^{-1}.[4] It is worth pointing out that the sensitivity of these LPG fibres is not as high when compared to other fibre sensors (such as gold coated tilted Bragg gratings, lossy mode resonance sensors, etc.), but here the point was to prove the effectiveness and reliability of the deposition of antifouling terpolymer brush (ATB) onto the LPG fibre by using a well-established sensing platform and a simple glassy substrate where ATB can be grafted.

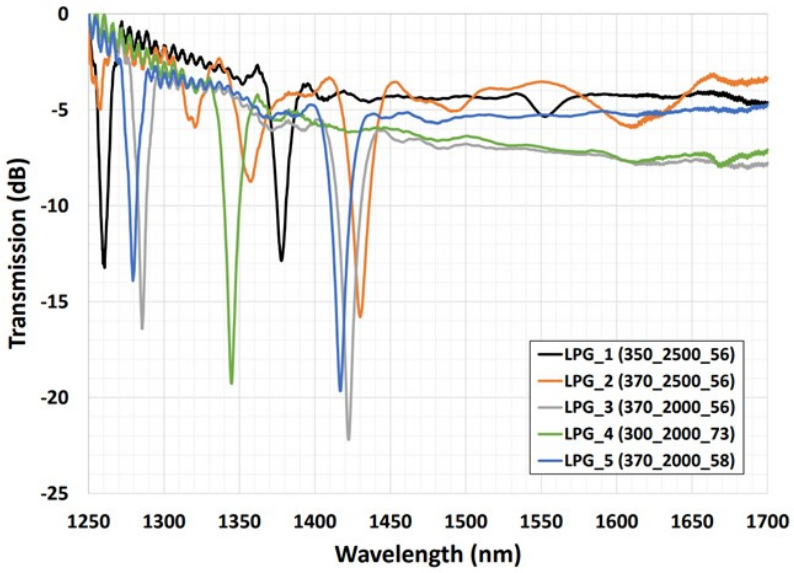

Fig. S1. Transmission spectra of 5 different LPG fibres before the deposition of terpolymer nano-brush.

Preparation of terpolymer nano-brushes

Random terpolymer nano-brushes, as shown in Fig. S2, were synthesized using surface-initiated atom transfer radical polymerization (SI ATRP) based on an optimized procedure published previously.[5] The preparation of the initiator self-assembled monolayer (SAM) differs for two different substrates: LPG fibres and gold-coated BK7 glass slides used as reference substrates. For the LPG fibres, the initial steps involved cleaning the fibres with acetone, followed by sonication in isopropanol and ultrapure water for 20 min each. Subsequently, they were treated in UV-ozone cleaner for 30 min. After that, the fibres were immersed into 1mM solution of bromo-silanes ($(MeO)_3$-Si-$(CH_2)_{11}$-Br) in heptane for 30 min to form an initiator SAM. In case of the gold-coated substrates, the glass slides with 50 nm Au layer were firstly cleaned in UV-ozone cleaner for 30 min, followed by rinsing with ultrapure water and ethanol. Immediately after cleaning, the slides were immersed in an initiator solution of 1mM 11-mercaptoundecyl-2-bromo-2-methylpropanoate in ethanol and allowed to rest in a dark place at room temperature for 2 days to form an initiator SAM.

In the next step, the SAM-coated LPG fibres (or gold-coated substrates) were rinsed with ethanol, dried with a stream of nitrogen, and carefully placed into a custom-made polymerization system. Prior to the polymerization process, methanol and ultrapure water were degassed through six freeze-pump-thaw cycles. The catalyst solution was prepared as follows: under a nitrogen atmosphere, 2.7 mL of degassed methanol was transferred to a Schlenk flask containing CuCl (38.0 mg), $CuCl_2$ (11.4 mg), and Me_4cyclam (131.4 mg). The mixture was sonicated for 5 min to ensure the dissolution of all solid components. Monomers SBMAA (0.187 g, 3 mol%), CBMAA (1.034 g, 20 mol%), and HPMAA (2.353 g, 77 mol%) were dissolved in 5.2 mL of degassed ultrapure water and 17.9 mL of degassed methanol in a separate Schlenk flask and stirred. Once the components were completely dissolved, the catalyst solution was injected into the monomer solution using a

gastight syringe. The resulting polymerization mixture was then added into the reactor containing the substrates with the initiator SAMs. Polymerization was conducted at room temperature for 2 h. Finally, after the polymerization the substrates were rinsed with ultrapure water and kept in PBS at 6 °C until needed.

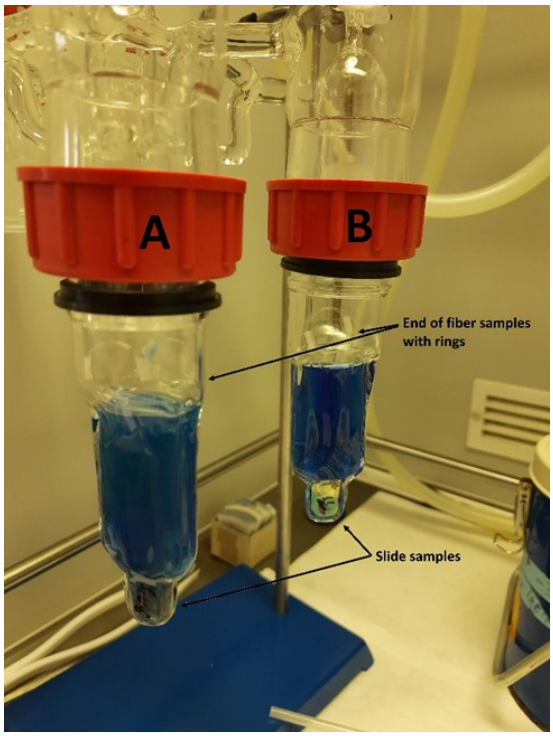

Fig. S2. Photograph of the two reactors A and B filled with the polymerization mixture, each reactor contains two slides and two fibres.

Fig. S3. Schematic representation of terpolymer architecture on a glass substrate, consisting of 77 mol % pHPMAA, 20 mol % pCBMAA and 3 mol % pSBMAA.

Step-by-step protocol for label-free experiments

Before the measurement, the LPG fibre was rinsed with ultrapure water, dried using a stream of air, and fixed inside the microfluidic system. In the first part of the experiment, the fibre was rehydrated by injection of ultrapure water and PBS for 30 min, followed by the EDC/NHS activation, functionalization of ATB with mouse IgG antibodies and AEAA deactivation as described for the fluorescence-based immunoassay. Finally, the optical fibre was rinsed with ultrapure water for 5 min and then washed with PBS for 30 min, both at a flow rate of 30 µL min^{-1}, to achieve a stable baseline. Then, 10% blood plasma (diluted in PBS, previously annealed to 37 °C and subsequently cooled to room temperature) was injected for 10 min as a negative control at the beginning of the detection part, followed by 10 min washing with PBS. The fouling level was determined by measuring the difference between the PBS baseline before plasma injection and the PBS baseline established 10 min after the plasma injection. Finally, the secondary anti-mouse IgG antibodies spiked in diluted plasma were introduced in increasing concentrations (0.01, 0.1, 1, and 10 µg mL^{-1}), each injection followed by 10 min washing with PBS.

Preparation of Eudragit-coated and functionalized LPG fibre

For label-free optical experiment shown in Fig. 5c the Eudragit-coated LPG fibre was prepared according to a previously described procedure.[6, 7] The sensitive region of a clean LPG fibre was immersed in 2 mM (0.04% w/v) Eudragit L 100 in ethanol for 1 min, and then it was left to dry for about 15 min until the solvent completely evaporated. After the copolymer deposition, the fibre was placed inside the thermo-stabilized microfluidic system and the measurement assay was performed similarly to the label-free experiments on ATB-coated LPG fibres as described above. Eudragit L 100 copolymer provides carboxyl functional groups, which enable covalent binding of biorecognition elements onto the fibre sensing surface. In the experiment performed on the Eudragit-coated LPG fibre, the 0.1% bovine serum albumin (BSA) in PBS was used for surface passivation after the immobilization of IgG antibodies (20 min, 12.6 µL min^{-1}), followed by rinsing with PBS for 10 min (30 µL min^{-1}).

Infrared reflection-absorption spectroscopy (IRRAS) and spectroscopic ellipsometry (SE)

The dimensions and material of the optical fibres make it impossible to measure the properties of polymer brushes by iS50 FTIR spectrometer or VASE spectroscopic ellipsometer directly on them. The spectra of ATB on a control gold substrate is shown in Fig. S4. The spectrum shows characteristic absorptions of all functional groups of the ATB. The Amide I and II bands of HPMAA, CBMAA and SBMAA have a common maximum at 1651 cm^{-1} and 1529 cm^{-1}, respectively. Due to a low content of CBMAA the absorption of ionized carboxyl group appears as a shoulder of the Amide I band at 1610 cm^{-1}; a week band at 1728 cm^{-1} indicates the presence of some non-ionized carboxyl groups. Sulfo group of SBMAA is manifested by the absorption at 1040 cm^{-1} and due to its very low content as a shoulder at 1211 cm^{-1} of a stronger band at 1203 cm^{-1}.

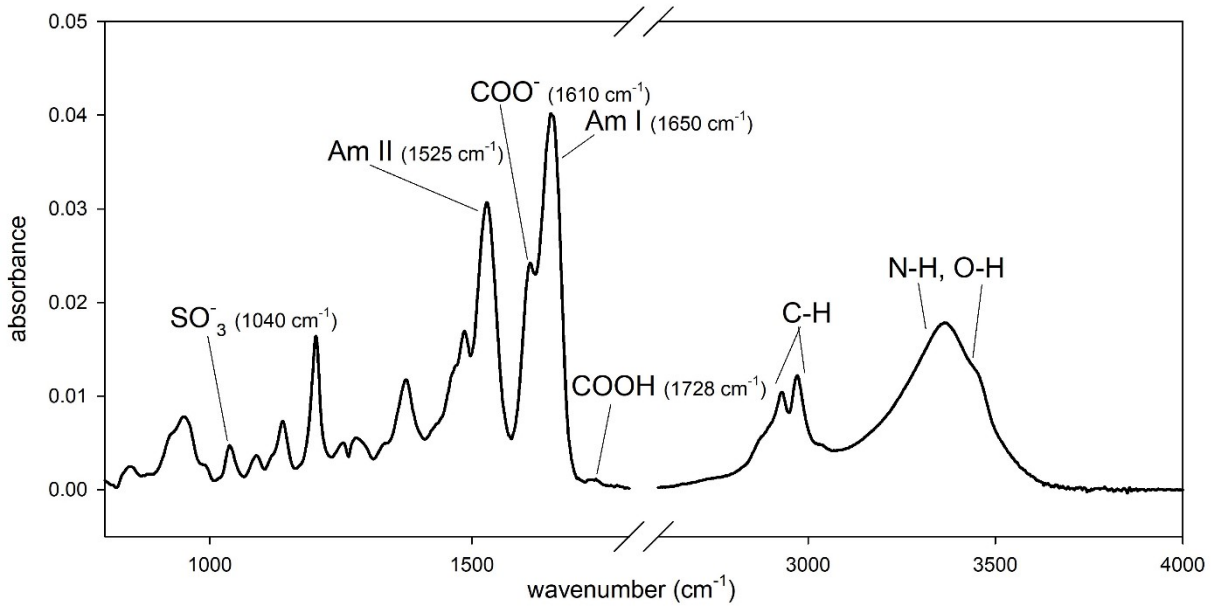

Fig. S4. IRRAS spectrum of terpolymer nano-brush on a control gold substrate.

The thickness of the ATB measured in air and water and the swelling ratio is shown in the Table S1. The errors shown stem from the fit of the ellipsometric data.

Table S1. Thickness and swelling of ATB measured by spectroscopic ellipsometry on a control gold substrate.

Sample	Dry thickness (nm)	Wet thickness (nm)	Swelling
ATB on control gold substrate	25.7 ± 0.5	79.5 ± 0.8	3.09 ± 0.07

Surface plasmon resonance (SPR)

In the first part of the SPR experiment, the binding capacity of ATB was determined by functionalization of the nano-brushes with IgG antibodies. The assay was performed similarly as the label-free experiments: firstly, the carboxyl groups of ATB were activated by EDC/NHS injection (15 µL min^{-1}, 20 min), followed by 2-min washing with ultrapure water, injection of anti-*E. coli* antibodies (50 µg mL^{-1}) in 5 mM HEPES pH 7 (15 µL min^{-1}, 20 min), again washing with water, and finally AEAA deactivation (15 µL min^{-1}, 30 min). In the second part, the fouling from plasma on ATB was assessed as follows: after a PBS baseline was established, undiluted human blood plasma (annealed at 37 °C and cooled down to room temperature, pH 7.9) was injected for 10 min, followed by 10 min washing with PBS, 5 min with PBS-NaCl, and another 10 min with PBS (all at 30 µL min^{-1}). The fouling levels were assessed as the difference between PBS baseline before plasma injection and achievement of PBS, resp. PBS-NaCl, baseline 10 min after PBS-NaCl injection.

SPR sensorgram is shown in Fig. S5. Fouling from undiluted plasma on ATB was 7.6 ng cm^{-2} in PBS, resp. 5.9 ng cm^{-2} after washing in buffer with a higher ionic strength (PBS-NaCl). The binding level on ATB was 182 ng cm^{-2}. These SPR data confirmed excellent antifouling behaviour and an expected binding capacity of the ATB coating used in this study.

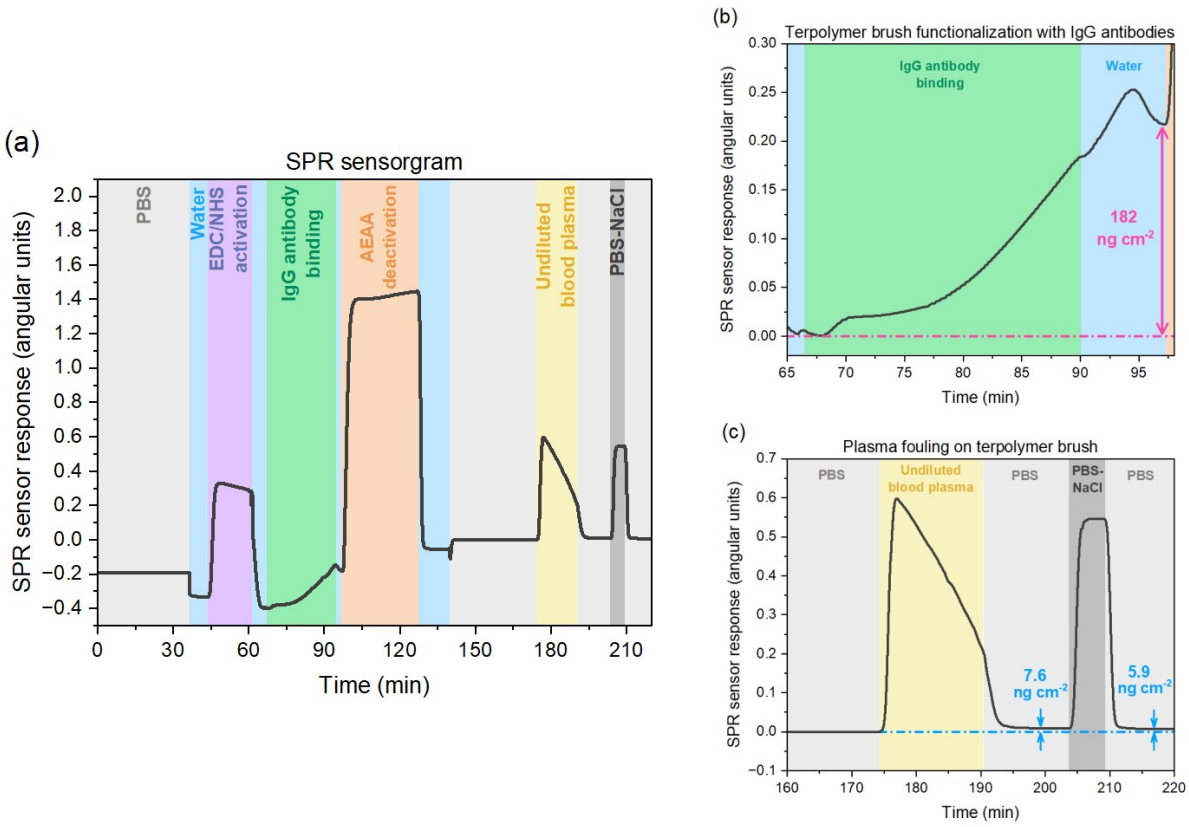

Fig. S5. SPR sensorgram of an experiment performed on ATB-coated control substrate: (a) Full sensorgram; (b) Detail of functionalization step with anti-*E. coli* antibodies; (c) Detail of fouling from undiluted human blood plasma.

Contact angle measurement

The wettability of ATB was determined by static contact angle of 17.8 ° ± 2.4 °, indicating strong hydrophilic behaviour of the nano-brush. Static contact angle analysis was executed with a drop of ultrapure water with a volume of 5.0 µL, loaded at a speed of 30 µL min^{-1}. The contact angles were determined using a Tangent 2 fitting model. Three chips were evaluated with three repetitions. The values are presented as the average of all measurements (including both right and left sides), and standard deviations were calculated.

Energy-dispersive X-ray spectroscopy (EDS)

Table S2. EDS analysis of three selected areas on bare optical fibre (area 1 shown in Fig. 3a).

Element	Area 1 (%)	Error (%)	Area 2 (%)	Error (%)	Area 3 (%)	Error (%)	Average (%)	Error (%)
C K	**3**	**14**	**12**	**11**	**9**	**11**	**8**	**12**
O K	**53**	**5**	**34**	**6**	**41**	**5**	**43**	**5**
Al K	**8**	**4**	**21**	**3**	**21**	**3**	**17**	**3**

Si K	**36**	**3**	**32**	**3**	**28**	**3**	**32**	**3**
Mg K	1	9	2	5	2	5	2	6
C/Si	**0.1**		**0.4**		**0.3**		**0.3**	

Table S3. EDS analysis of two selected areas on ATB-coated LPG fibre (shown in Fig. 3b).

Element	Area 1 (%)	Error (%)	Area 2 (%)	Error (%)
C K	**46**	**16**	**63**	**14**
N K	**3**	**81**	**4**	**42**
O K	**21**	**12**	**12**	**14**
Al K	**20**	**5**	**15**	**5**
Si K	**11**	**6**	**6**	**6**
Cu L	1	20	0	21
C/Si	**4**		**11**	

Table S4. EDS analysis of area 2 on ATB-coated LPG fibre (shown in Fig. 3c).

Element	Spot 1 (%)	Error (%)	Spot 2 (%)	Error (%)	Spot 3 (%)	Error (%)	Spot 4 (%)	Error (%)	Spot 5 (%)	Error (%)
C K	**51**	**18**	**47**	**18**	**50**	**18**	**67**	**13**	**59**	**16**
N K	**5**	**52**	**8**	**35**	**6**	**50**	**6**	**35**	**5**	**43**
O K	**12**	**16**	**12**	**15**	**12**	**15**	**9**	**15**	**11**	**15**
Al K	**27**	**5**	**26**	**5**	**27**	**5**	**13**	**5**	**17**	**5**
Si K	**4**	**10**	**4**	**10**	**4**	**9**	**4**	**7**	**7**	**7**
Cl K	0	51	1	24	1	29	0	41	0	41
Cu L	1	21	1	22	1	23	0	24	1	23
Ag L	1	41	1	40	1	40	0	38	0	57
C/Si	**12**		**12**		**13**		**17**		**8**	

References

1. F. Chiavaioli, F. Baldini and C. Trono, *Fibers*, 2017, **5**, 29.

2. T. Erdogan, *J. Opt. Soc. Am. A*, 1997, **14**, 1760-1773.

3. F. Chiavaioli, C. A. J. Gouveia, P. A. S. Jorge and F. Baldini, *Biosensors*, 2017, **7**, 23.

4. F. Chiavaioli, C. Trono, A. Giannetti, M. Brenci and F. Baldini, *J. Biophotonics*, 2014, **7**.

5. M. Forinová, A. Pilipenco, I. Víšová, N. S. Lynn, Jr., J. Dostálek, H. Mašková, V. Hönig, M. Palus, M. Selinger, P. Kočová, F. Dyčka, J. Štěrba, M. Houska, M. Vrabcová, P. Horák, J. Anthi, C.-P. Tung, C.-M. Yu, C.-Y. Chen, Y.-C. Huang, P.-H. Tsai, S.-Y. Lin, H.-J. Hsu, A.-S. Yang, A. Dejneka and H. Vaisocherová-Lísalová, *ACS Appl. Mater. Interfaces*, 2021, **13**, 60612-60624.

6. F. Chiavaioli, D. Santano Rivero, I. Del Villar, A. B. Socorro-Leránoz, X. Zhang, K. Li, E. Santamaría, J. Fernández-Irigoyen, F. Baldini, D. L. A. van den Hove, L. Shi, W. Bi, T. Guo, A. Giannetti and I. R. Matias, *Adv. Photonics Res.*, 2022, **3**, 2200044.

7. F. Chiavaioli, P. Zubiate, I. Del Villar, C. R. Zamarreño, A. Giannetti, S. Tombelli, C. Trono, F. J. Arregui, I. R. Matias and F. Baldini, *ACS Sens.*, 2018, **3**, 936-943.